JCAMECH

Vol. 48, No. 1, June 2017, pp 89-98
DOI: 10.22059/jcamech.2017.233633.143

Elastic analysis of functionally graded rotating thick cylindrical pressure vessels with exponentially-varying properties using power series method of Frobenius

Mahboobeh Gharibi [1], Mohammad Zamani Nejad [1*], Amin Hadi[2]

[1] *Mechanical Engineering Department, Yasouj University, P. O. Box: 75914-353, Yasouj, Iran.*

[2] *School of Mechanical Engineering, University of Tehran, Tehran, Iran.*

Received: 20 May. 2017, Accepted: 19 June. 2017

Abstract

Based on the Frobenius series method, stresses analysis of the functionally graded rotating thick cylindrical pressure vessels (FGRTCPV) are examined. The vessel is considered in both plane stress and plane strain conditions. All of the cylindrical shell properties except the Poisson ratio are considered exponential function along the radial direction. The governing Navier equation for this problem is determined, by employing the principle of the two dimensional elastic theories. This paper presents a closed-form analytical solution for the Navier equation of FGRTCPV as the novelty of the present paper. Moreover, a finite element (FE) model is developed for comparison with the results of the Frobenius series method. This comparison demonstrates that the results of the Frobenius series method are accurate. Finally, the effect of some parameters on stresses analysis of the FGRTCPV is examined. In order to investigate the inhomogeneity effect on the elastic analysis of functionally graded rotating thick cylindrical pressure vessels with exponentially-varying properties, values of the parameters have been set arbitrary in the present study. The presented outcomes illustrate that the inhomogeneity constant provides a major effect on the mechanical behaviors of the exponential FG thick cylindrical under pressure.

Keywords: Rotating thick cylinder, Pressure vessel, Functionally graded material, Exponentially, Power series method of Frobenius Introduction

1. Introduction

Functionally Graded Materials (FGMs) have been developing rapidly in the past two decades [1]. A group of composite materials are called FGM that mechanical properties vary continuously from one surface to another [2]. This type of material is a new class of advanced composite materials [3-8], in which the microstructural details are spatially varied through smooth and continuous distribution of the reinforcement phase [9]. Structures made of FGMs are designed in order to optimize their performance in one or more directions depending upon the loads anticipated to act on them [10]. A number of different

[*] Corresponding Author. Tel.: +98 7433221711; fax.: +98 7433221711
E-mail address: m_zamani@yu.ac.ir , m.zamani.n@gmail.com (M.Z. Nejad)

papers, which are considered various aspects of FGM, have been published in recent years [11-22]. Thick wall pressure vessels are commonly used in industry for storage and transportation of

liquids and gases when designed as tanks. The displacement and stresses analysis of pressurized hollow cylinder or disk made FG materials are presented by Horgan and Chan. [23]. These researchers assumed that the modulus of elasticity is a power law function of the radial direction. In this paper, the Poisson's ratio was constant. Tutuncu and Ozturk [24], perused the stress analysis in the FG pressure vessels. This paper provided an exact solution for displacements of FG spherical and cylindrical pressure vessels. Shi et al. [25], Presented a scheme to investigating FG structure. They offered that FG structure can convert to the N-layered homogeneous elastic hollow cylinder. Tutuncu [26], by using power series method investigates stress analysis of cylindrical pressure vessels made of exponentially FG materials. The exponential FG cylindrical and spherical pressure vessels are presented by Chen and Lin [27]. Assuming the shear modulus in the radial direction is vary based on a power law relation or an exponential function, Batra and Nie [28], obtained analytically plane strain infinitesimal deformations of a non- asymmetrically loaded hollow cylinder, on the other hand, an eccentric cylinder composed of a linear elastic isotropic and incompressible functionally graded material. Using the Airy stress function, Nie and Batra [29], investigated of a FG cylinder under both axisymmetric and non-axisymmetric loads. In another study, using the Airy stress function, an exact solution for a functionally graded hollow cylinder under plane strain condition are presented by Nie and Batra [30]. Callioglu, Bektas, and Sayer [31] obtained a closed-form solutions for elastic analysis of FG annular rotating disks. Material parameters except Poisson's ratio, have the power-law dependence on the radial direction, Fatehi and Nejad [32], presented a parametric analysis for purely elastic analysis of rotating FGM thick hollow cylindrical shells as per plane strain condition. Using a elastoperfectly plastic material and Tresca's model as the yield criterion, Nejad et al. [13], studied elasto-plastic analysis in an functionally graded rotating disk. They presented an analytical solution in terms of radial displacement.

A semi-analytical solution for stresses analysis of FG rotating thick cylindrical pressure vessels with variable thickness are performed by Nejad et al. [33].

This paper presents the elastic analysis of FG thick cylindrical pressure vessels with exponentially-varying properties using the Frobenius series method. Considering all studies in the given field, there are no works carried out so far related to this issue. Eventually, a numerical solution based on finite element program ANSYS for verification of results is performed.

2. Formulation of problem

In this section, the distribution of displacement and stress in a rotating FGM thick hollow cylindrical pressure vessel in the conditions of both plane strain and plane stress will be calculated. Consider a rotating thick hollow cylinder with an internal radii a, and an external radii b, exposed to an internal uniform pressure P, which is axisymmetric. The cylinder is assumed under a constant angular velocity ω (Figure 1).

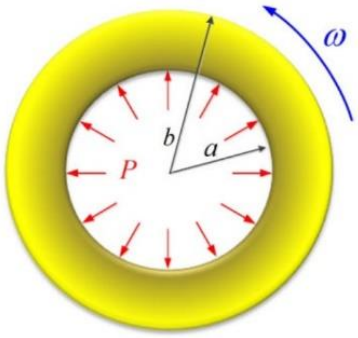

Figure 1: Cross section of FGM thick-walled cylindrical pressure vessel.

The material properties except for the Poisson's ratio of the cylinder are assumed as an exponential function of radial direction as follows [34]:

$$E = E_i e^{\beta_1\left(\frac{r-a}{b-a}\right)},\ \rho = \rho_i e^{\beta_2\left(\frac{r-a}{b-a}\right)}, \tag{1}$$

where E_i and ρ_i are Young's modulus and density in inner surface, respectively. β_1 and β_2 take negative or positive values, and represent the property of the FGMs, which is called the inhomogeneous constant hereafter.

In the case of symmetrical deformation, the equilibrium equation takes the below form

$$\frac{d}{dr}(r\sigma_{rr}) - \sigma_{\theta\theta} + \rho\omega^2 r^2 = 0. \tag{2}$$

In the case of small deformation, the strain components is as follow

$$\varepsilon_{rr} = \frac{du}{dr},\ \varepsilon_{\theta\theta} = \frac{u}{r}, \tag{3}$$

where, u is the displacement in the radial-direction.

The general relations for a non-homogeneous isotropic cylindrical shell are

$$\begin{bmatrix}\sigma_{rr}\\ \sigma_{\theta\theta}\end{bmatrix}=E\begin{bmatrix}A & B\\ B & A\end{bmatrix}\begin{bmatrix}\varepsilon_{rr}\\ \varepsilon_{\theta\theta}\end{bmatrix}, \tag{4}$$

where A and B are function of Poisson's ratio ν as follow:

$$\textit{Plane stress}: \begin{cases} A=\dfrac{1}{1-\nu^2} \\ B=\dfrac{\nu}{1-\nu^2} \end{cases}$$

$$\textit{Plane Strain}: \begin{cases} A=\dfrac{1-\nu}{(1+\nu)(1-2\nu)} \\ B=\dfrac{\nu}{(1+\nu)(1-2\nu)} \end{cases} \tag{5}$$

Using Eqs. (1) to (4), the Navier Equation is

$$r^2u_r''+r(1+hr)u_r'-(1-h\nu_1 r)u_r =$$

$$=-fr^3e^{(\beta_2-\beta_1)\frac{r-a}{b-a}}. \tag{6}$$

The following equation is established by assumption $\beta_1=\beta_2=\beta$.

$$r^2u_r''+r(1+hr)u_r'-(1-h\nu_1 r)u_r=-fr^3. \tag{7}$$

where

$$\nu_1=\frac{\nu}{1-\nu},\quad h=\frac{\beta}{b-a},\quad f=\frac{\rho_i\omega^2}{AE_i}. \tag{8}$$

Using Frobenius method [35], Eq. (7) can be solved as follow:

$$u_r=\sum_{n=0}^{\infty}a_n r^{n+s}. \tag{9}$$

Substituting Eq. (9) into Eq. (7)

$$a_0\left(s^2-1\right)r^s+\sum_{n=0}^{\infty}\Big[\left((n+s+1)^2-1\right)a_{n+1}+ \\ +h(n+s+\nu_1)a_n\Big]r^{n+s+1}=-fr^3. \tag{10}$$

The solution of Eq. (7) is as follows

$$u_r=u_h+u_p \tag{11}$$

where u_h and u_p are homogeneous and particular solutions, respectively. Homogeneous solution is obtained by solving Eq. (12)

$$a_0(s-1)(s+1)r^s+\sum_{n=0}^{\infty}\Big[\left((n+s+1)^2-1\right)a_{n+1} \\ +h(n+s+\nu_1)a_n\Big]r^{n+s+1}=0. \tag{12}$$

Since $a_0\neq 0$

$$(s-1)(s+1)=0\rightarrow(s_1=+1\ ,\ s_2=-1). \tag{13}$$

Eq. (13) is called the indicial equation for Eq. (7). It is observed that the roots of the indicial equation are differ by an integer, thus only one of the solutions is in the form of Eq. (9).

In the Eq. (12), the recursive relation is as follow:

$$a_{n+1}=-\frac{h(n+s+\nu_1)}{(n+s+1)^2-1}a_n. \tag{14}$$

Expansion of the recurrence relation gives the coefficients a_n function of a_0 and Gamma functions as follows:

$$a_n=\frac{(-1)^n\Gamma(n+s+\nu_1)\Gamma(s+2)^2a_0h^n}{s(s+1)\Gamma(s+\nu_1)\Gamma(n+s)\Gamma(n+s+2)}. \tag{15}$$

The first solution of Eq. (7) determined for $(s_1=+1\,,\,a_0=1)$.

$$u_1=r+\sum_{n=1}^{\infty}a_n(s_1)r^{n+1}, \tag{16}$$

where

$$a_n(s_1)=\frac{2(-1)^n\Gamma(n+\nu_1+1)}{\Gamma(\nu_1+1)\Gamma(n+1)\Gamma(n+3)}h^n. \tag{17}$$

For the second root $(s_2=-1)$, the second solution of Eq. (7) obtained in the form

$$u_2=Qu_1\ln(r)+r^{s_2}\left[1+\sum_{n=1}^{\infty}C_n(s_2)r^n\right], \tag{18}$$

where

$$\begin{cases} Q=lim_{s\rightarrow s_2}(s-s_2)a_N(s)=\dfrac{h^2\nu_1(1-\nu_1)}{2}, \\ C_n(s_2)=\dfrac{d}{ds}\Big[(s-s_2)a_n(s)\Big]. \end{cases} \tag{19}$$

Assume that

$$L=(s+1)a_n(s)= \\ =\frac{(-1)^n\Gamma(n+s+\nu_1)\Gamma(s+2)^2}{s\Gamma(s+\nu_1)\Gamma(n+s)\Gamma(n+s+2)}h^n. \tag{20}$$

hence

$$L_{s_2=-1}=\frac{(-1)^{n-1}\,\Gamma(n+\nu_1-1)}{n!(n-2)!\,\Gamma(\nu_1-1)}h^n. \tag{21}$$

and

$$\frac{d}{ds}\Big[ln(L)\Big]\Big|_{s=s_2}=1+2\frac{\Gamma'(1)}{\Gamma(1)}+\frac{\Gamma'(n+\nu_1-1)}{\Gamma(n+\nu_1-1)}- -\frac{\Gamma'(\nu_1-1)}{\Gamma(\nu_1-1)}-\frac{\Gamma'(n-1)}{\Gamma(n-1)}-\frac{\Gamma'(n+1)}{\Gamma(n+1)}. \tag{22}$$

The $\Psi(z)$ is defined as follows

$$\Psi(z)=\frac{\Gamma'(z)}{\Gamma(z)}, \tag{23}$$

Substituting Eq. (23) into Eq. (22)

$$\frac{d}{ds}\Big[ln(L)\Big]|_{s=s_2}=1+2\Psi(1)+\Psi(n+\nu_1-1)- -\Psi(\nu_1-1)-\Psi(n-1)-\Psi(n+1). \tag{24}$$

Hence, the $C_n(s_2)$ will be as follows

$$C_n(s_2)=\frac{(-1)^{n-1}\,\Gamma(n+\nu_1-1)h^n}{n!(n-2)!\,\Gamma(\nu_1-1)}\times \times\Big[1+2\Psi(1)+\Psi(n+\nu_1-1)- -\Psi(\nu_1-1)-\Psi(n-1)-\Psi(n+1)\Big]. \tag{25}$$

Finally, the homogeneous solution of Eq. (7) is

$$u_h=c_1u_1+c_2u_2=c_1\left[r+\sum_{n=1}^{\infty}a_n(s_1)r^{n+1}\right]+c_2\left[Q\left[r+\sum_{n=1}^{\infty}a_n(s_1)r^{n+1}\right]ln(r)+\left[r^{-1}+\sum_{n=1}^{\infty}C_n(s_2)r^{n-1}\right]\right]. \tag{26}$$

In order to obtaining particular solution of Eq. (7), in Eq. (12), it is considered that $s_3=3$

$$a_0=-\frac{f}{8},\ a_{n+1}=\frac{-h(n+\nu_1+3)}{(n+4)^2-1}a_n. \tag{27}$$

Where

$$a_n(s_3)=\frac{6(-1)^{n+1}\,\Gamma(n+\nu_1+3)\,fh^n}{\Gamma(\nu_1+3)\Gamma(n+3)\Gamma(n+5)}. \tag{29}$$

The particular solution of Eq. (7) is

$$u_p=-\frac{1}{8}fr^3+\sum_{n=1}^{\infty}a_n(s_3)r^{n+3}, \tag{28}$$

Thus, the solution of Eq. (7) is expressed as

$$u_r=c_1u_1+c_2u_2+u_p=c_1\left[r+\sum_{n=1}^{\infty}a_n(s_1)r^{n+1}\right]++c_2\left[Q\left[r+\sum_{n=1}^{\infty}a_n(s_1)r^{n+1}\right]ln(r)+\left[r^{-1}+\sum_{n=1}^{\infty}C_n(s_2)r^{n-1}\right]\right] +\left[-\frac{1}{8}fr^3+\sum_{n=1}^{\infty}a_n(s_3)r^{n+3}\right]. \tag{30}$$

Substitution of Eq. (30) into first Eqs. (3-4)

$$\sigma_{rr}=AEc_1\left[1+\nu_1+\sum_{n=1}^{\infty}Fa_n(s_1)r^n\right]+AEc_2\left[Q\Big[(1+\nu_1)ln(r)+1\Big]-\frac{1-\nu_1}{r^2}+Q\sum_{n=1}^{\infty}\Big[F\,ln(r)+1\Big]a_n(s_1)r^n+ +\sum_{n=1}^{\infty}GC_n(s_2)r^{n-2}\right]+AE\left[-\frac{(3+\nu_1)f}{8}r^2+\sum_{n=1}^{\infty}Ha_n(s_3)r^{n+2}\right], \tag{31}$$

where

$$F=n+1+\nu_1,\ G=n-1+\nu_1,\ H=n+3+\nu_1. \tag{32}$$

The constants c_1 and c_2 are determined using the boundary conditions $\sigma_{rr}(r=a)=-P$ and $\sigma_{rr}(r=b)=0$

$$c_1=\frac{-1}{V_{1b}(m-t)}\left[\frac{P}{AE_i}+V_{3a}-tV_{3b}\right],\qquad c_2=\frac{1}{V_{2b}(m-t)}\left[\frac{P}{AE_i}+V_{3a}-mV_{3b}\right] \tag{33}$$

where

$$\begin{cases}V_{1a}=1+\nu_1+\sum_{n=1}^{\infty}Fa_n(s_1)a^n,\\ V_{1b}=1+\nu_1+\sum_{n=1}^{\infty}Fa_n(s_1)b^n.\end{cases} \tag{34}$$

$$\begin{aligned}V_{2a}&=Q\left[(1+\nu_1)ln(a)+1\right]-\frac{1-\nu_1}{a^2}+Q\sum_{n=1}^{\infty}\left[F\,ln(a)+1\right]a_n(s_1)a^n+\sum_{n=1}^{\infty}GC_n(s_2)a^{n-2},\\ V_{2b}&=Q\left[(1+\nu_1)ln(b)+1\right]-\frac{1-\nu_1}{b^2}+Q\sum_{n=1}^{\infty}\left[F\,ln(b)+1\right]a_n(s_1)b^n+\sum_{n=1}^{\infty}GC_n(s_2)b^{n-2}\end{aligned} \tag{35}$$

$$\begin{cases}V_{3a}=-\frac{(3+\nu_1)f}{8}a^2+\sum_{n=1}^{\infty}Ha_n(s_3)a^{n+2},\\ V_{3b}=-\frac{(3+\nu_1)f}{8}b^2+\sum_{n=1}^{\infty}Ha_n(s_3)b^{n+2}.\end{cases} \tag{36}$$

Therefore, the radial deformation, radial and circumferential stresses of the exponential FGM thick rotating cylindrical pressure vessel are obtained as

$$\begin{aligned}u_r=&\frac{P+(V_{3a}-mV_{3b})AE_i}{V_{2b}(m-t)AE_i}\times\left[\left(Q\,ln(r)-\frac{V_{2b}}{V_{1b}}\frac{P+(V_{3a}-tV_{3b})AE_i}{P+(V_{3a}-mV_{3b})AE_i}\right)\times\left[r+\sum_{n=1}^{\infty}a_n(s_1)r^{n+1}\right]+\frac{1}{r}+\sum_{n=1}^{\infty}C_n(s_2)r^{n-1}\right]\\ &-\frac{1}{8}fr^3+\sum_{n=1}^{\infty}a_n(s_3)r^{n+3}.\end{aligned} \tag{37}$$

$$\begin{aligned}\sigma_{rr}=&AE_ie^{\beta\frac{r-a}{b-a}}\left[\frac{P+(V_{3a}-mV_{3b})AE_i}{V_{2b}(m-t)AE_i}\times\left[-\frac{V_{2b}}{V_{1b}}\frac{P+(V_{3a}-tV_{3b})AE_i}{P+(V_{3a}-mV_{3b})AE_i}\times\left[1+\nu_1+\sum_{n=1}^{\infty}Fa_n(s_1)r^n\right]\right.\right.\\ &\left.\left.+Q\left[(1+\nu_1)ln(r)+1\right]-\frac{1-\nu_1}{r^2}+Q\sum_{n=1}^{\infty}\left[F\,ln(r)+1\right]a_n(s_1)r^n+\sum_{n=1}^{\infty}GC_n(s_2)r^{n-2}-\frac{(3+\nu_1)f}{8}r^2+\sum_{n=1}^{\infty}Ha_n(s_3)r^{n+2}\right]\right.\end{aligned} \tag{38}$$

$$\begin{aligned}\sigma_{\theta\theta}=&AE_ie^{\beta\frac{r-a}{b-a}}\left[\frac{P+(V_{3a}-mV_{3b})AE_i}{V_{2b}(m-t)AE_i}\times\left[-\frac{V_{2b}}{V_{1b}}\frac{P+(V_{3a}-tV_{3b})AE_i}{P+(V_{3a}-mV_{3b})AE_i}\times\left[1+\nu_1+\sum_{n=1}^{\infty}F^*a_n(s_1)r^n\right]+\right.\right.\\ &\left.\left.Q\left[(1+\nu_1)ln(r)+\nu_1\right]+\frac{1-\nu_1}{r^2}+Q\sum_{n=1}^{\infty}\left[F^*\,ln(r)+\nu_1\right]a_n(s_1)r^n+\sum_{n=1}^{\infty}G^*C_n(s_2)r^{n-2}-\frac{(1+3\nu_1)f}{8}r^2+\sum_{n=1}^{\infty}H^*a_n(s_3)r^{n+2}\right]\right.\end{aligned} \tag{39}$$

where

$$m=\frac{V_{1a}}{V_{1b}},\ t=\frac{V_{2a}}{V_{2b}}. \tag{40}$$

and

$$F^*=\nu_1(n+1)+1,\ G^*=\nu_1(n-1)+1,\\ H^*=\nu_1(n+3)+1 \tag{41}$$

3. Results and discussion

Consider a rotating cylindrical shell in plane stress problem under the inner uniform pressure of 40 MPa. The cylinder has the internal and external radii of 40 cm and 60 cm, respectively. Additionally, it is considered that values of the Poisson's ratio, ν, internal Young's modulus E_i and internal density ρ_i, are 0.3, 200 GPa, and 7860 kg/m^3, respectively. For a comparative examine on numerical evaluation of this problem, a geometry specimen is patterned applying commercial finite element code, ANSYS. Because of the geometrical symmetry in the cylinder, just a quarter of the specimen geometry in the finite element model was considered. To be able to represent the non-homogeneous specimen, an 8-node axisymmetric quadrilateral element was applied. The variation in material properties was applied by 20 layers, with each layer having a constant value of material properties, for modeling of FGM cylindrical pressure vessel. Figure 2 demonstrates the meshing of a quarter of the specimen geometry. The case study for rotating cylinder is administered at two sections:

- Angular velocity is constant and inhomogeneous constant is variable.
- Angular velocity is variable and inhomogeneous constant is fixed.

3.1. Section 1: The angular velocity has a constant value of 100 rad/s*:*

Figure 3 reveals the distribution of Young's modulus in the r direction. It is considerable that Young's modulus increases, since the value of β expands. Figure 4 reveals the distribution of radial deformation versus the dimensionless r direction. It is evident that at the same situation, the radial deformation declines as β grows. The distribution of compressive radial stress versus dimensionless r direction is shown in Figure 5. It is observed that the radial stress raises for larger values of β. The circumferential stress versus dimensionless radial direction for various values of β is drawn in Figure 6.

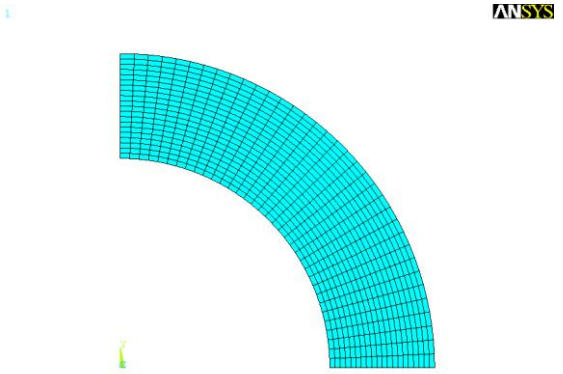

Figure. 2. Finite element mesh region.

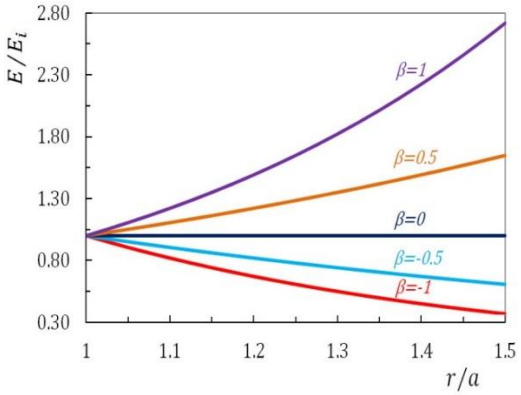

Figure 3. Radial distribution of Young's modulus

The purpose should be observed using this figure that at the same condition, approximately, for $\beta<1.2$, the value of the circumferential stress reduces as β raises although for $\beta>1.2$, this situation is reversed. Moreover, the circumferential stress reduces versus the r direction for approximately $\beta<0.5$, but, for almost $\beta>0.5$, the circumferential stress increases. Furthermore, for $\beta\approx0.5$, the circumferential stress remains nearly uniform versus the radius of the cylinder. The issue could be a important factor for control of optimum stress. For the goal of examining the stress distribution versus r direction, the von Mises equivalent stress versus the r direction, is drawn in

Figure 7. It is observed that at all considered conditions, the equivalent stress for $\beta = 0.75$ remains nearly uniform along the radius of the cylinder. It means that this parameter can be considered as a significant element in terms of controlling stresses. The von Mises equivalent stress raises for $\beta > 0.75$, as the radius increases whereas for $\beta < 0.75$, it lessens. Furthermore, It can be seen that by increasing, distribution of material properties will increase.

In Figures 8 to 10, the amounts of all radial, circumferential and von Mises equivalent stresses are determined in the case of $\beta = 0.75$. These figures display the stress distribution in 20 layers of thick cylindrical pressure vessels.

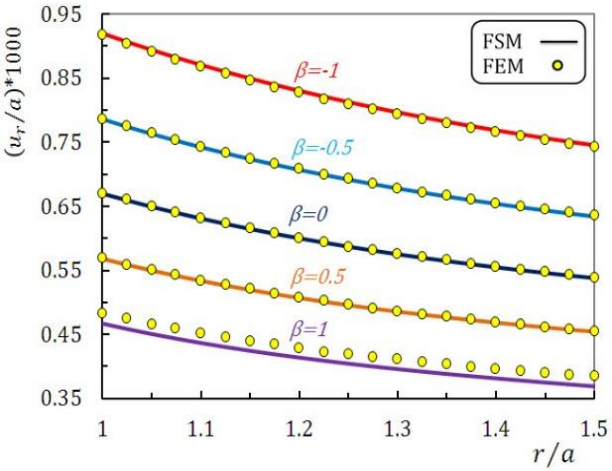

Figure 4. Radial distribution of radial displacement

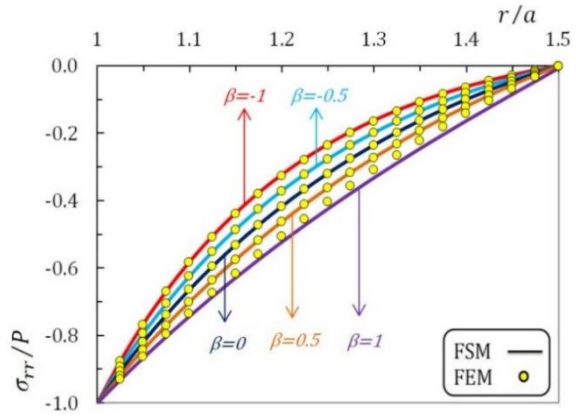

Figure 5. Radial distribution of radial stress

3.2. Section 2: The inhomogeneous constant has a fixed amount of $\beta = 0.5$.

Figure 11 shows the distribution of tensile radial displacement along the normalized radial direction. It is apparent that at the same position, the radial deformation raises as ω increases. The distribution of radial stress versus *r* direction is shown in Figure 12. It is seen that for larger values of ω, the stress declines. According to Figure 13, the radial stress is compressive for all values of angular velocity except for $\omega > 225$ and $r/a > 1.25$. This figure reveals the radial distribution of circumferential stress. For all values of angular velocity, the circumferential stress remains nearly uniform versus *r* direction. The matter could be a significant factor in terms of controlling optimum stress. For the purpose of studying the stress distribution along the hollow cylinder radius, in Figure 14, the von Mises equivalent stress is plotted in the radial direction. The equivalent stress increases as ω grows.

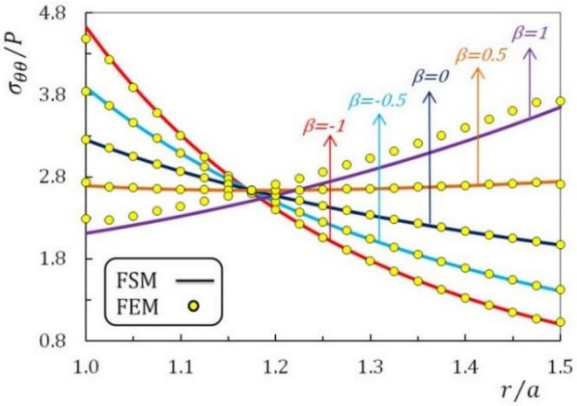

Figure 6. Radial distribution of circumferential stress

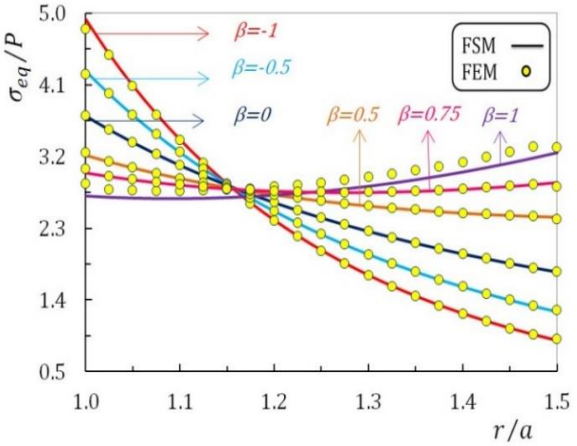

Figure 7. Radial distribution of von Mises equivalent stress

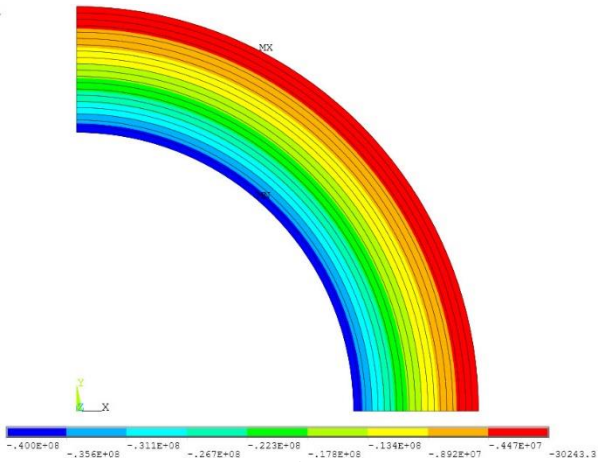

Figure 8. Radial stress obtained from ANSYS code in a rotating FGM cylindrical pressure vessel ($\beta = 0.75$)

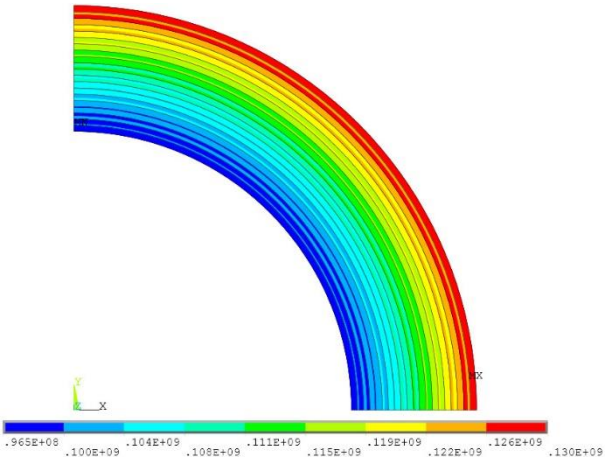

Figure 9. Circumferential stress obtained from ANSYS code in a rotating FGM cylindrical pressure vessel ($\beta = 0.75$)

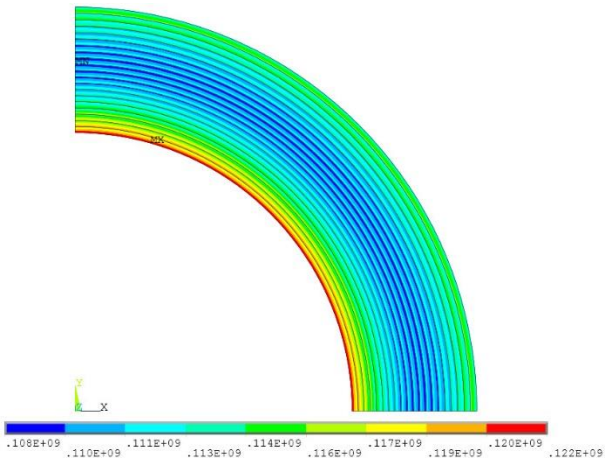

Figure 10. von Mises equivalent stress obtained from ANSYS code in a rotating FGM cylindrical pressure vessel ($\beta = 0.75$)

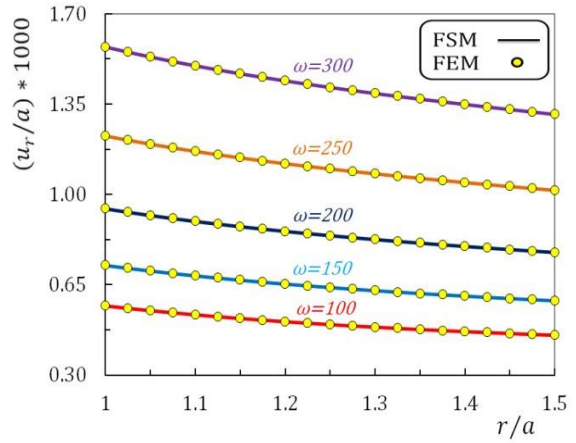

Figure 11. Radial distribution of radial displacement

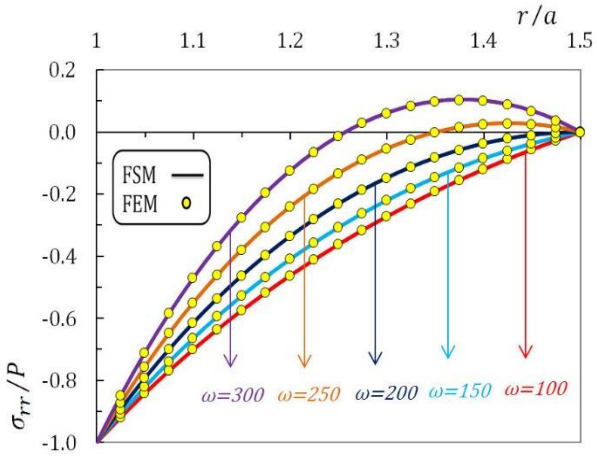

Figure 12. Radial distribution of radial stress

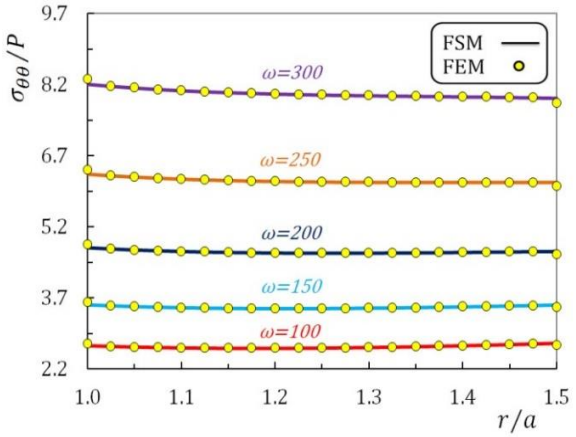

Figure 13. Radial distribution of circumferential stress

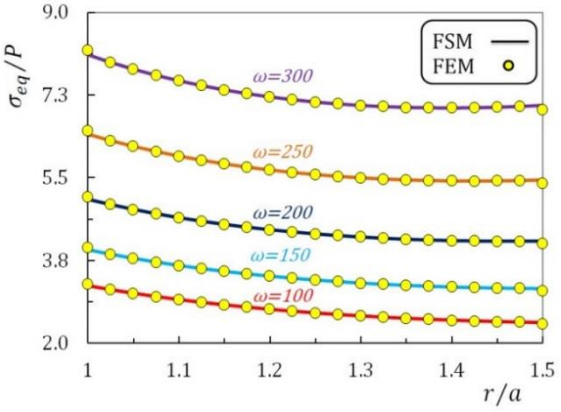

Figure 14. Radial distribution of von Mises equivalent stress

4. Conclusion

It is apparent that analytical solutions to simplified versions of real engineering problems are important. The Frobenius series technique is really a strong strategy for obtaining answers of particular differential equations that arise in applications. According to fundamental equations of elasticity and ultizing FSM, analytic solutions are derived for stresses and the displacements of rotating exponential FGM thick hollow cylindrical under pressure. Using this, profiles are plotted for various values of inhomogeneity constant and angular velocity for the radial deformation, radial and circumferential stresses, as a function of *r* direction. Also, this research presents a numerical solution employing a commercial finite elements code, ANSYS. Excellent agreement is discovered between the analytic solutions and the solutions based on ANSYS finite element code. The presented outcomes illustrate that the inhomogeneity constant provides a major effect on the mechanical behaviors of the exponential FG thick cylindrical under pressure.

References

[1] K. Khorshidi, A. Bakhsheshy, Free Natural Frequency Analysis of an FG Composite Rectangular Plate Coupled with Fluid using Rayleigh–Ritz Method, *Mechanics of Advanced Composite Structures*, Vol. 1, No. 2, pp. 131-143, 2014.

[2] A. M. Zenkour, Dynamical bending analysis of functionally graded infinite cylinder with rigid core, *Applied Mathematics and Computation*, Vol. 218, No. 17, pp. 8997-9006, 2012.

[3] A. Hadi, A. Rastgoo, A. Daneshmehr, F. Ehsani, Stress and strain analysis of functionally graded rectangular plate with exponentially varying properties, Indian Journal of Materials Science, Vol. 2013, 2013.

[4] M. Mohammadi, M. Safarabadi, A. Rastgoo, A. Farajpour, Hygro-mechanical vibration analysis of a rotating viscoelastic nanobeam embedded in a visco-Pasternak elastic medium and in a nonlinear thermal environment, *Acta Mechanica*, Vol. 227, No. 8, pp. 2207-2232, 2016.

[5] M. Goodarzi, M. Mohammadi, A. Farajpour, M. Khooran, Investigation of the effect of pre-stressed on vibration frequency of rectangular nanoplate based on a visco pasternak foundation, *Journal of Solid Mechanics*, Vol. 6, pp. 98-121, 2014.

[6] S. R. Asemi, M. Mohammadi, A. Farajpour, A study on the nonlinear stability of orthotropic single-layered graphene sheet based on nonlocal elasticity theory, *Latin American Journal of Solids and Structures*, Vol. 11, No. 9, pp. 1515-1540, 2014.

[7] M. R. Farajpour, A. Rastgoo, A. Farajpour, M. Mohammadi, Vibration of piezoelectric nanofilm-based electromechanical sensors via higher-order non-local strain gradient theory, *Micro & Nano Letters*, Vol. 11, No. 6, pp. 302-307, 2016.

[8] M. Mohammadi, A. Farajpour, M. Goodarzi, H. Mohammadi, Temperature effect on vibration analysis of annular graphene sheet embedded on visco-pasternak foundation, *J. Solid Mech*, Vol. 5, pp. 305-323, 2013.

[9] B. S. Aragh, E. B. Farahani, A. N. Barati, Natural frequency analysis of continuously graded carbon nanotube-reinforced cylindrical shells based on third-order shear deformation theory, *Mathematics and Mechanics of Solids*, Vol. 18, No. 3, pp. 264-284, 2013.

[10] J. Dryden, R. Batra, Material tailoring and moduli homogenization for finite twisting deformations of functionally graded Mooney-Rivlin hollow cylinders, *Acta Mechanica*, Vol. 224, No. 4, pp. 811-818, 2013.

[11] A. Daneshmehr, A. Rajabpoor, A. Hadi, Size dependent free vibration analysis of nanoplates made of functionally graded materials based on nonlocal elasticity theory with high order theories, *International Journal of Engineering Science*, Vol. 95, pp. 23-35, 2015.

[12] M. Z. Nejad, A. Hadi, Non-local analysis of free vibration of bi-directional functionally graded Euler–Bernoulli nano-beams, *International Journal of Engineering Science*, Vol. 105, pp. 1-11, 2016.

[13] M. Z. Nejad, A. Rastgoo, A. Hadi, Exact elasto-plastic analysis of rotating disks made of functionally graded materials, *International Journal of Engineering Science*, Vol. 85, pp. 47-57, 2014.

[14] M. Z. Nejad, A. Hadi, A. Rastgoo, Buckling analysis of arbitrary two-directional functionally graded Euler–Bernoulli nano-beams based on nonlocal elasticity theory, *International Journal of Engineering Science*, Vol. 103, pp. 1-10, 2016.

[15] M. Z. Nejad, A. Hadi, Eringen's non-local elasticity theory for bending analysis of bi-directional functionally graded Euler–Bernoulli nano-beams, *International Journal of Engineering Science*, Vol. 106, pp. 1-9, 2016.

[16] M. Kahrobaiyan, M. Rahaeifard, S. Tajalli, M. Ahmadian, A strain gradient functionally graded

Euler–Bernoulli beam formulation, *International Journal of Engineering Science*, Vol. 52, pp. 65-76, 2012.

[17] Z. Mazarei, M. Z. Nejad, A. Hadi, Thermo-elasto-plastic analysis of thick-walled spherical pressure vessels made of functionally graded materials, *International Journal of Applied Mechanics*, Vol. 8, No. 04, pp. 1650054, 2016.

[18] M. Z. Nejad, G. Rahimi, Deformations and stresses in rotating FGM pressurized thick hollow cylinder under thermal load, *Scientific Research and Essays*, Vol. 4, No. 3, pp. 131-140, 2009.

[19] M. Jabbari, M. Z. Nejad, M. Ghannad, Thermo-elastic analysis of axially functionally graded rotating thick cylindrical pressure vessels with variable thickness under mechanical loading, *International journal of engineering science*, Vol. 96, pp. 1-18, 2015.

[20] M. Jabbari, M. Z. Nejad, M. Ghannad, Thermo-elastic analysis of axially functionally graded rotating thick truncated conical shells with varying thickness, *Composites Part B: Engineering*, Vol. 96, pp. 20-34, 2016.

[21] M. Nejad, A. Rastgoo, A. Hadi, Effect of Exponentially-Varying Properties on Displacements and Stresses in Pressurized Functionally Graded Thick Spherical Shells with Using Iterative Technique, *Journal of Solid Mechanics Vol*, Vol. 6, No. 4, pp. 366-377, 2014.

[22] M. Hosseini, M. Shishesaz, K. N. Tahan, A. Hadi, Stress analysis of rotating nano-disks of variable thickness made of functionally graded materials, *International Journal of Engineering Science*, Vol. 109, pp. 29-53, 2016.

[23] C. Horgan, A. Chan, The pressurized hollow cylinder or disk problem for functionally graded isotropic linearly elastic materials, *Journal of Elasticity*, Vol. 55, No. 1, pp. 43-59, 1999.

[24] N. Tutuncu, M. Ozturk, Exact solutions for stresses in functionally graded pressure vessels, *Composites Part B: Engineering*, Vol. 32, No. 8, pp. 683-686, 2001.

[25] Z. Shi, T. Zhang, H. Xiang, Exact solutions of heterogeneous elastic hollow cylinders, *Composite structures*, Vol. 79, No. 1, pp. 140-147, 2007.

[26] N. Tutuncu, Stresses in thick-walled FGM cylinders with exponentially-varying properties, *Engineering Structures*, Vol. 29, No. 9, pp. 2032-2035, 2007.

[27] Y. Chen, X. Lin, Elastic analysis for thick cylinders and spherical pressure vessels made of functionally graded materials, *Computational Materials Science*, Vol. 44, No. 2, pp. 581-587, 2008.

[28] R. Batra, G. Nie, Analytical solutions for functionally graded incompressible eccentric and non-axisymmetrically loaded circular cylinders, *Composite Structures*, Vol. 92, No. 5, pp. 1229-1245, 2010.

[29] G. Nie, R. Batra, Exact solutions and material tailoring for functionally graded hollow circular cylinders, *Journal of Elasticity*, Vol. 99, No. 2, pp. 179-201, 2010.

[30] G. Nie, R. Batra, Material tailoring and analysis of functionally graded isotropic and incompressible linear elastic hollow cylinders, *Composite structures*, Vol. 92, No. 2, pp. 265-274, 2010.

[31] H. Çallioğlu, N. B. Bektaş, M. Sayer, Stress analysis of functionally graded rotating discs: analytical and numerical solutions, *Acta Mechanica Sinica*, Vol. 27, No. 6, pp. 950-955, 2011.

[32] P. Fatehi, M. Z. Nejad, Effects of material gradients on onset of yield in FGM rotating thick cylindrical shells, *International Journal of Applied Mechanics*, Vol. 6, No. 04, pp. 1450038, 2014.

[33] M. Z. Nejad, M. Jabbari, M. Ghannad, Elastic analysis of axially functionally graded rotating thick cylinder with variable thickness under non-uniform arbitrarily pressure loading, *International Journal of Engineering Science*, Vol. 89, pp. 86-99, 2015.

[34] M. H. Sadd, 2009, *Elasticity: theory, applications, and numerics*, Academic Press,

[35] W. E. Boyce, R. C. DiPrima, C. W. Haines, 1969, *Elementary differential equations and boundary value problems*, Wiley New York.